Detection of very high energy gamma-ray emission from the gravitationally-lensed blazar QSO B0218+357 with the MAGIC telescopes

Ahnen et al. 2016
A&A, 595 (2016) A98

Astroparticle Physics with Gamma-rays

Thu, 11 May, 2017
Fiori Michele

Summary

1) Introduction

2) Observations and analysis

3) Influence of the lensing galaxy

4) Detection significance (MAGIC)

5) Temporal Results

6) Spectral Results

7) Broadband emission

8) EBL constrains

9) Conclusions

Introduction

- About 60 Blazars detected at energies >100 GeV, almost all at $z<0.5$.
- Observations of distant sources in VHE gamma-rays are difficult owing to strong absorption in the extragalactic background light. At a $z\sim1$ it results in a cut-off at energies of ~100 GeV.
- MAGIC Telescopes discovered VHE gamma-ray emission from QSO B0218+357 and PKS1441+25 at $z>0.9$.

Introduction

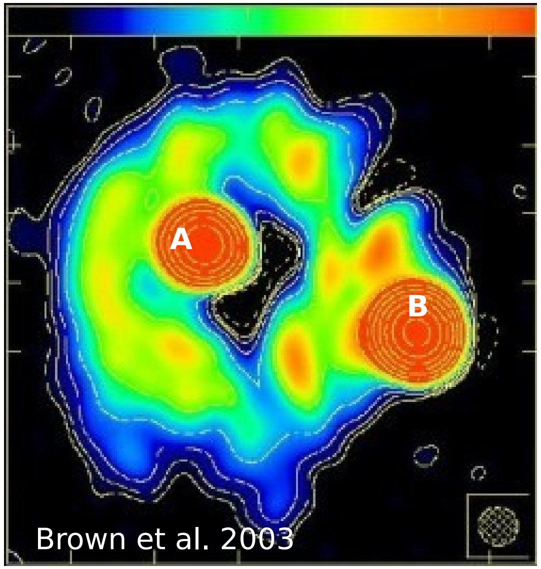

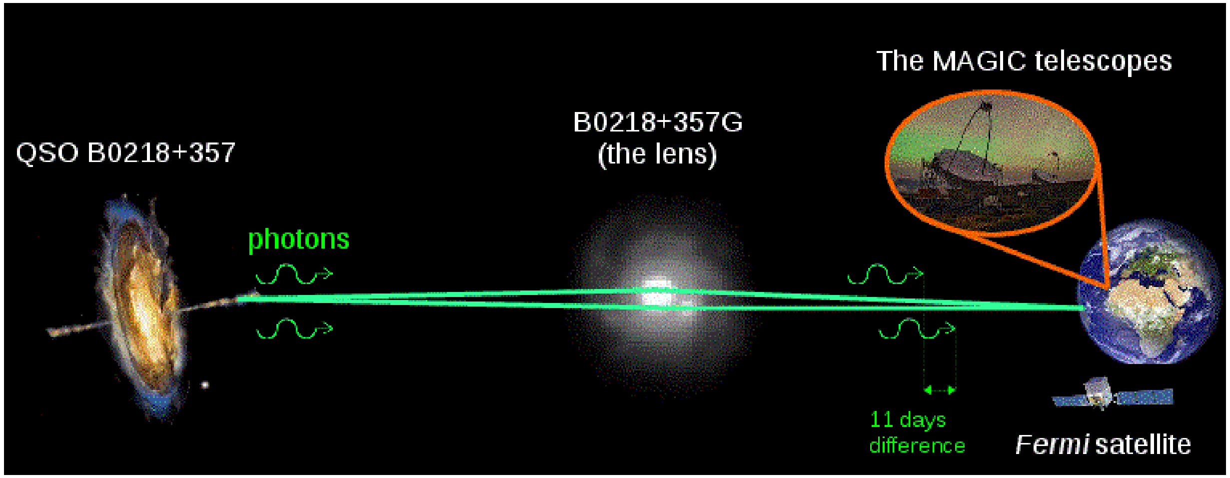

MAGIC Image credits: Daniel Lopez/IAC; Hubble image of B0218+357G credits: NASA/ESA; AGN image credits: NASA E/PO - Sonoma State University, Aurore Simonne

QSO B0218+35

Flat Spectrum Radio Quasar (FSRQ)

z_s=0.944+-0.002, z_l=0.68466+-0.00004

Two distinct component, a leading component (A) and a trailing component (B), with a time delay of 11,46+-0.16 days.

Value of the flux magnification ratio between the two component dependent on frequency.

Source went through a series of outburst in 2012 and in July 2014.

Observations and analysis

VHE - MAGIC

Observed only trailng component

23/07/2014-05/08/2014 (12.8h)

Zenith angle: 20°-43°

Standard data reduction

Energy threshold of 85 GeV

HE - *Fermi*-LAT

Flaring first observed with *Fermi*

11/07/2014-06/08/2014 (2.7 days ToO)

0.1-300 GeV

Data extracted from a 15° radius region

P7REP_SOURCE_V15

X-ray - *Swift*

Leading and trailing component

10 observation epochs, ~4.5 ks each

0.2-10 KeV

Data analysis with HEASoft V. 6.17, PC mode with ~0.02 ct/s

Optical - KVA

Observed only trailing component

24/07/2014-05/08/2014

Optical R-band

Differential Photometry Magnitude

Object very faint with ~19 mag, one image per night

Influence of the lensing galaxy

The interpretation of the QSO B0218+357 observations is not trivial due to the influence of the lensing galaxy and microlensing (by individual stars).

Variability of the flux magnification caused by microlensing is larger for smaller emission regions in the source → Gamma-ray emission expected from smaller region respect to the radio emission region

Flux ratio between the two images in radio is ~3.6 (μ_{lead}~2.7, μ_{trail}~0,7)

↓

Unaffected by microlensing!

Microlensing in HE and VHE energy ranges can significantly affect observed fluxes.

Fermi-LAT observations → Flux ratio higher! Microlensing affect more the leading image

The observed flux also are affected by absorption in the lensing galaxy.
In the optical band the leading image is weaker than the trailing image!

Results - Detection significance (MAGIC)

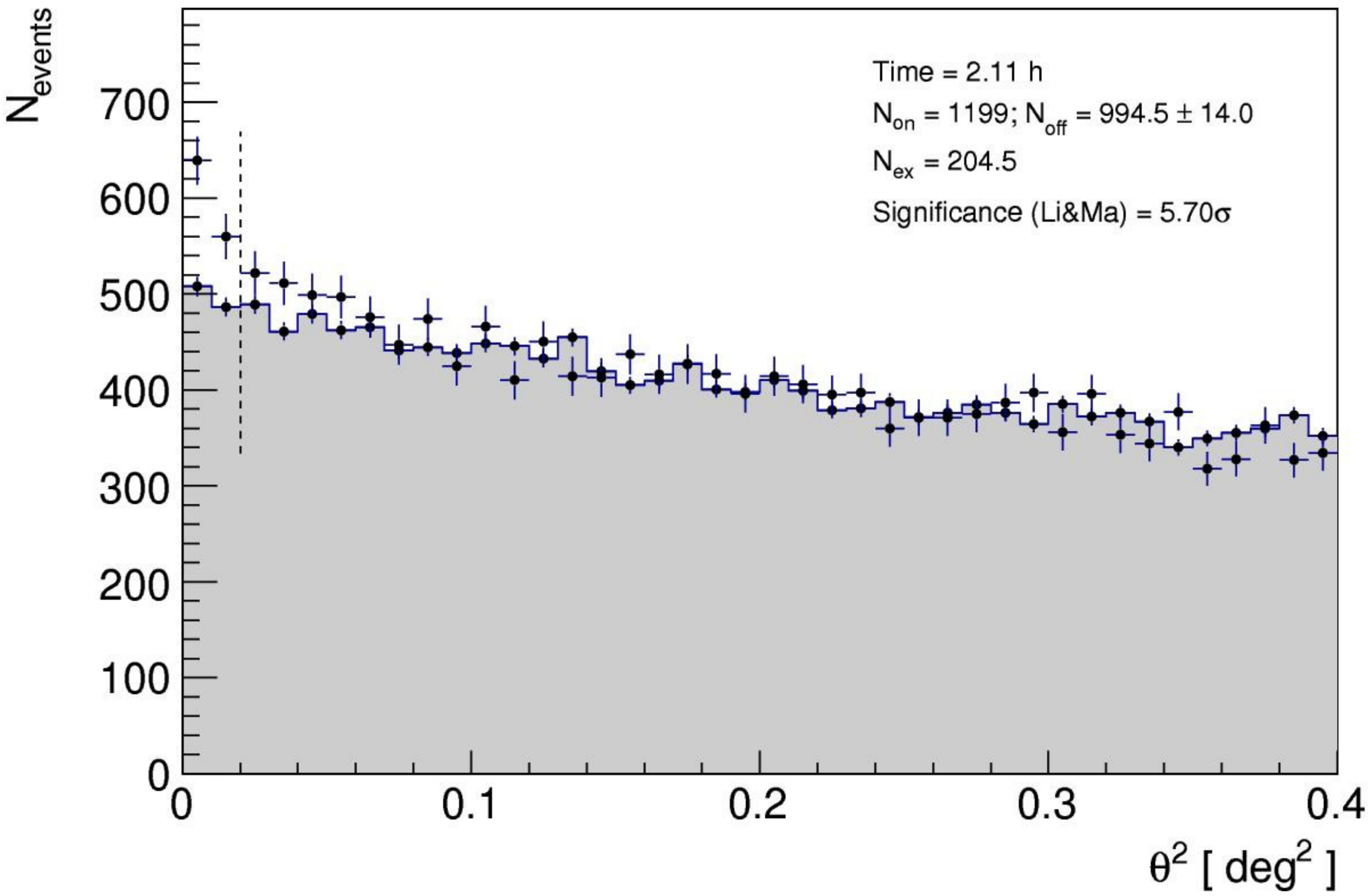

Distribution of the squared angular distance, θ^2, between the reconstructed source position and the nominal source position (points) or the background estimation position (shaded area). The vertical dashed line shows the value of θ^2 up to which the number of excess events and significance are computed.

Temporal Results

MAGIC

Gaussian function for fitting the peak position. Probability of 21%

Mean flux above 100 GeV (flaring nights):

$(5.8 \pm 1.6_{stat} \pm 2.4_{syst}) \times 10^{-11} cm^{-2} s^{-1}$

Large systematic errors due to the 15% uncertainty in the energy scale

Fermi-LAT

Minimun increasad at 0.3 GeV (to increase S/N)

Significant GeV emission detected both during the two flare (TS of 615 and 129)

GeV emission outside the flaring events marginally detected.

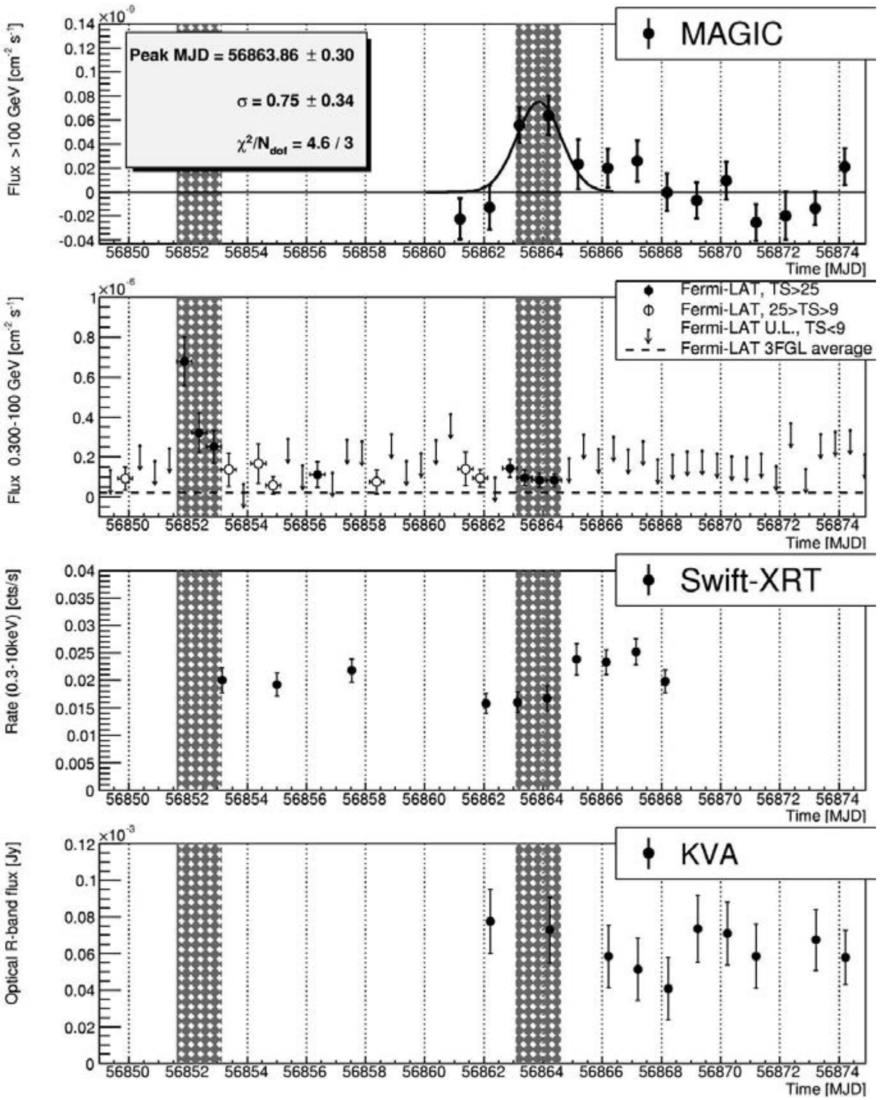

Temporal Results

Swift

Only a small hint of variability (costant fit probability 1,1%)

KVA

In all of the observation the source was fainter than 19 magnityude, resulting error bars relatively large!

No significant variability detected

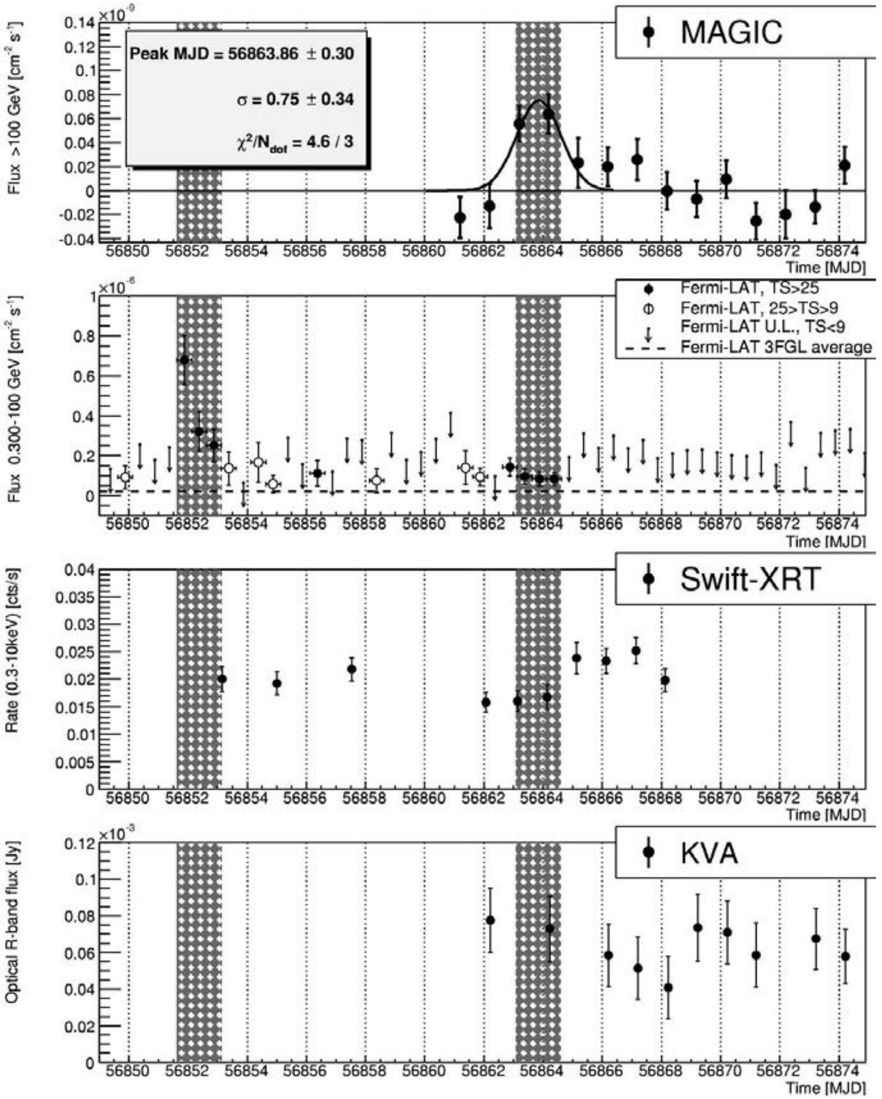

Spectral Results - MAGIC

SED obtained during the trailing flare and the reconstructed spectrum spans the energy range 65-175 GeV. Spectrum severely affected by the absorption of VHE gamma-rays in the EBL.

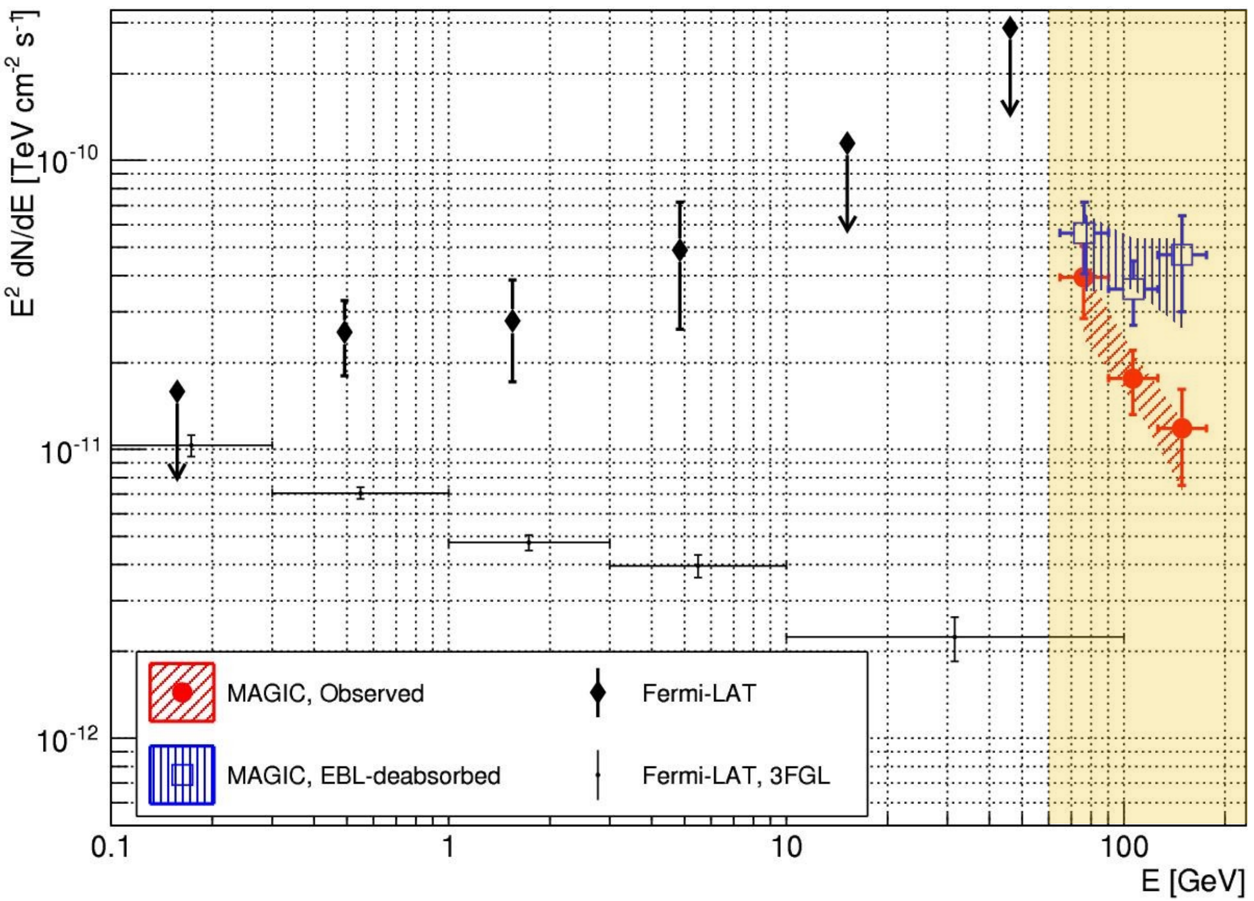

Spectral Results - MAGIC

$$\frac{dN}{dE} = f_0 \times \left(\frac{E}{100GeV}\right)^{-\gamma} [cm^{-2}s^{-1}TeV^{-1}]$$

$$f_0 = (2.0 \pm 0.4_{stat} \pm 0.9_{syst}) \times 10^{-9} cm^{-2}s^{-1}TeV^{-1}$$
$$\gamma = 3.80 \pm 0.61_{stat} \pm 0.20_{syst}$$

Observed

$$f_0 = (4.6 \pm 0.8_{stat} \pm 2.1_{syst}) \times 10^{-9} cm^{-2}s^{-1}TeV^{-1}$$
$$\gamma = 2.35 \pm 0.75_{stat} \pm 0.20_{syst}$$

EBL-deabsorbed

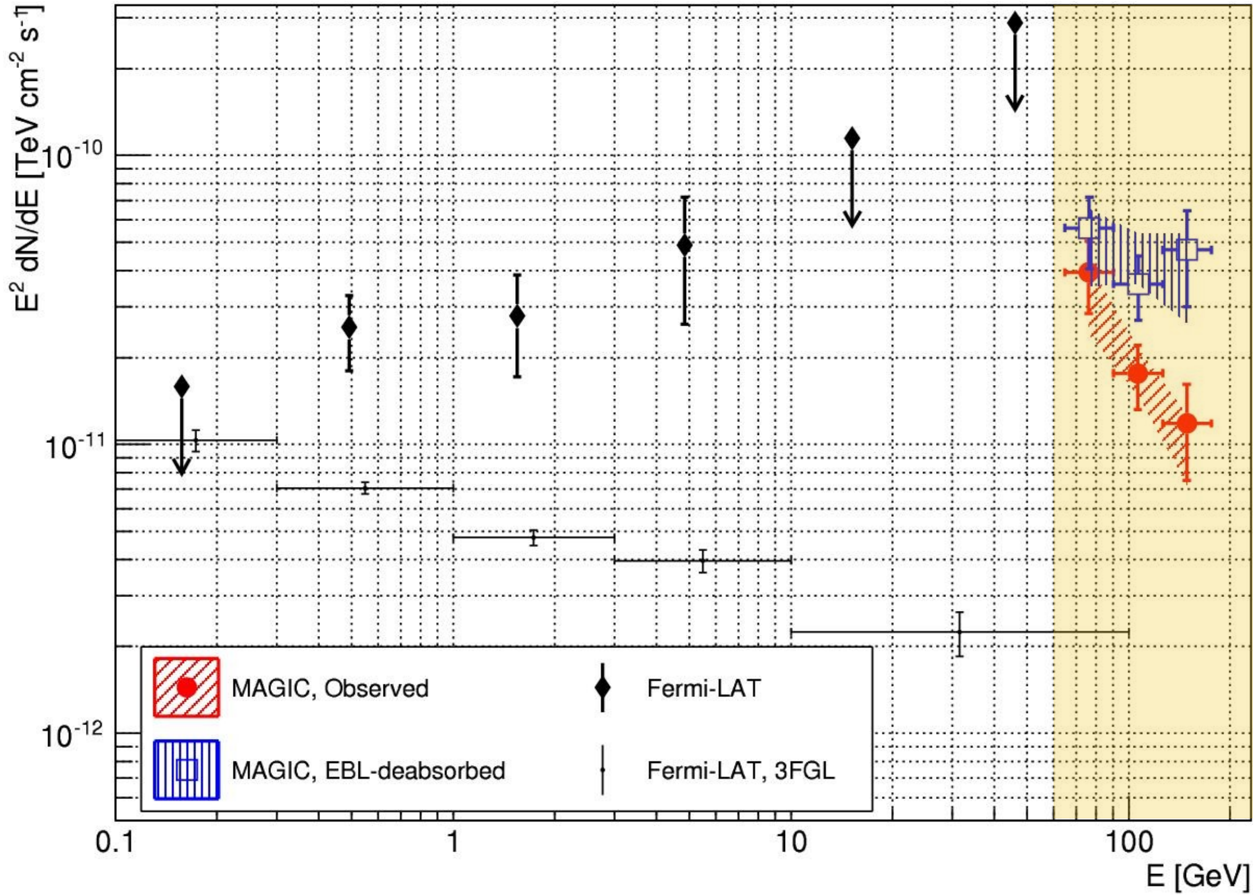

Spectral Results - *Fermi*-LAT

SED obtained during the trailing flare. Spectral index much harder than in the average state of this source (and also harder than the spectral index during the flare event in 2012).

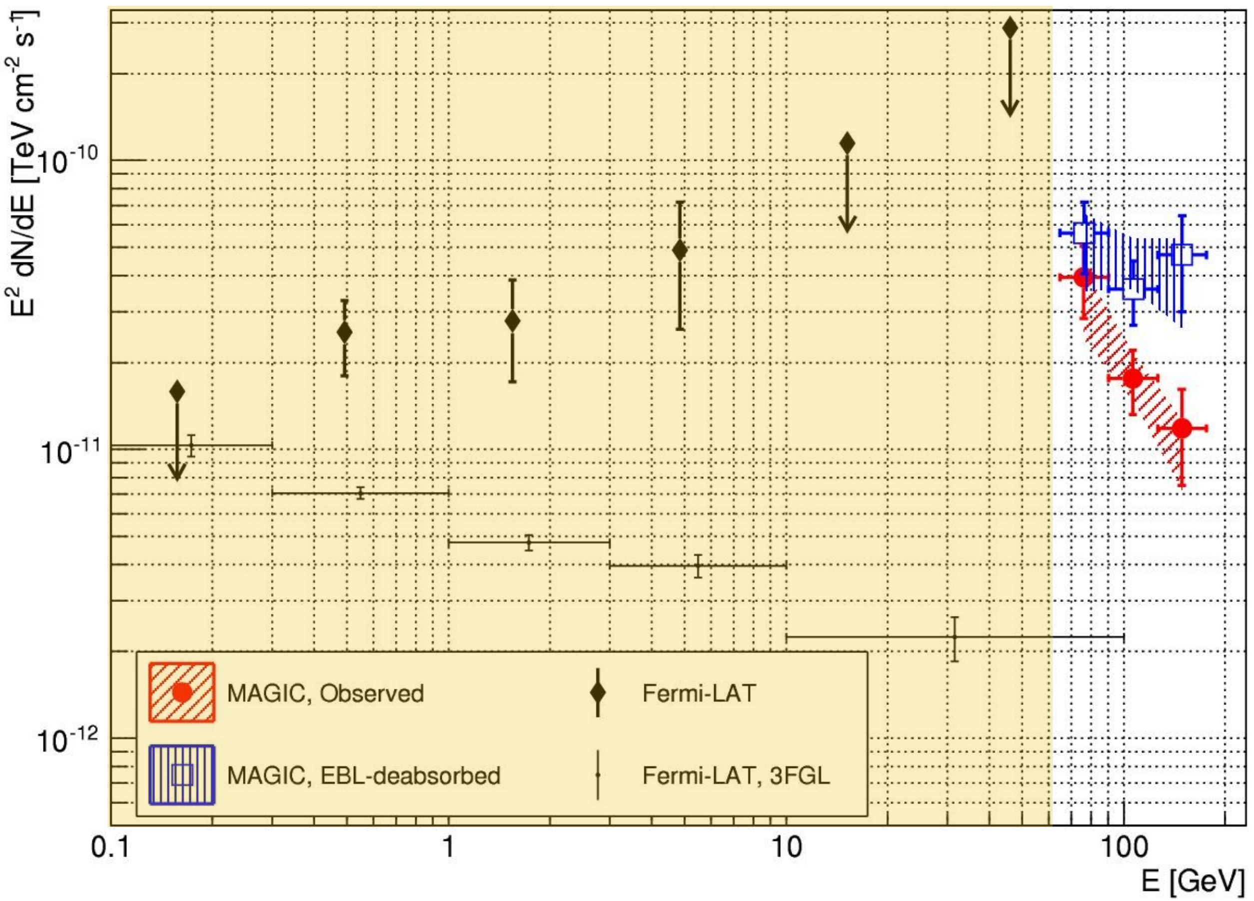

Spectral Results - *Fermi*-LAT

Leading flare

$$F_{>1GeV} = (6.7 \pm 1.0) \times 10^{-7} cm^{-2} s^{-1}$$

$$\gamma = 1.35 \pm 0.09$$

Trailing flare

$$F_{>1GeV} = (1.7 \pm 0.4) \times 10^{-7} cm^{-2} s^{-1}$$

$$\gamma = 1.6 \pm 0.1$$

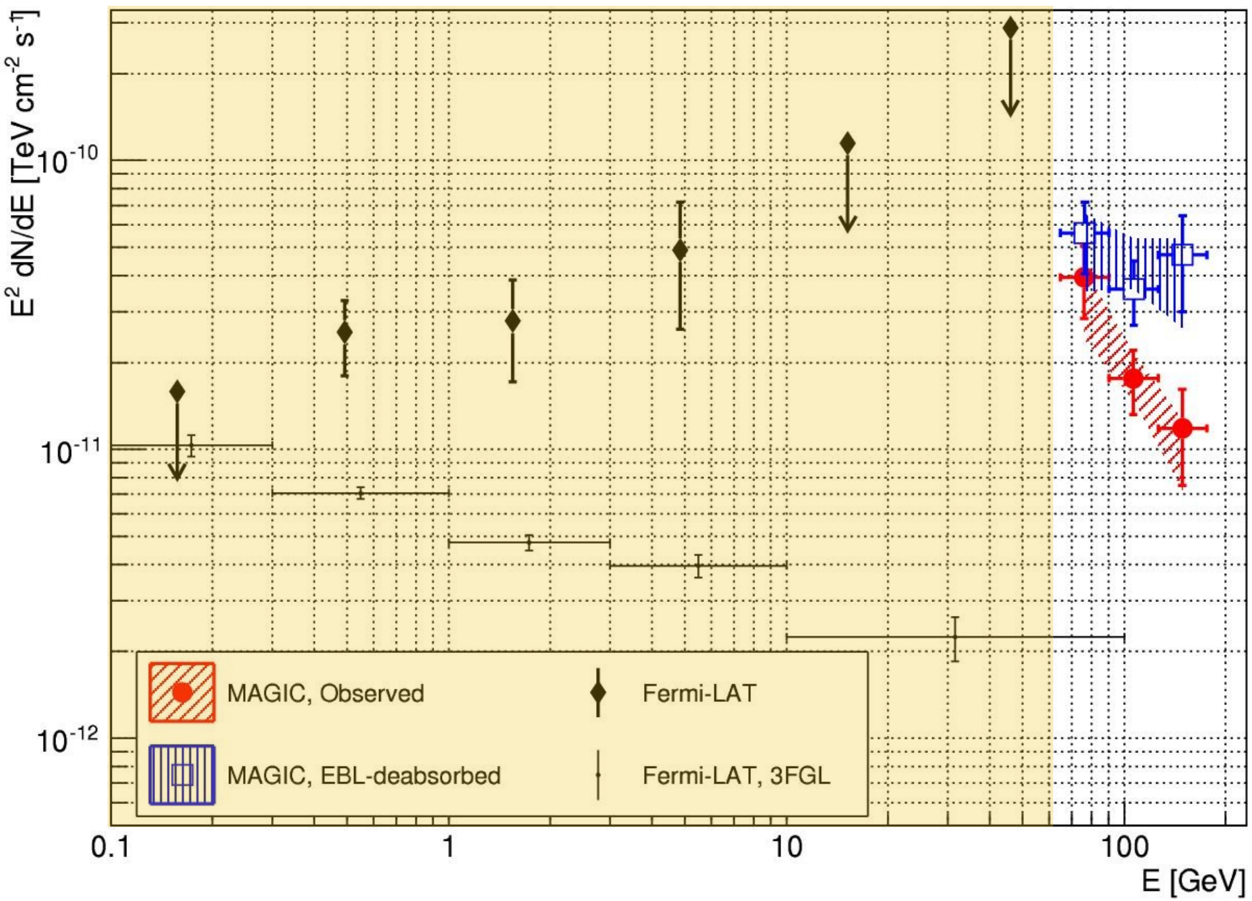

Spectral Results - *Swift*

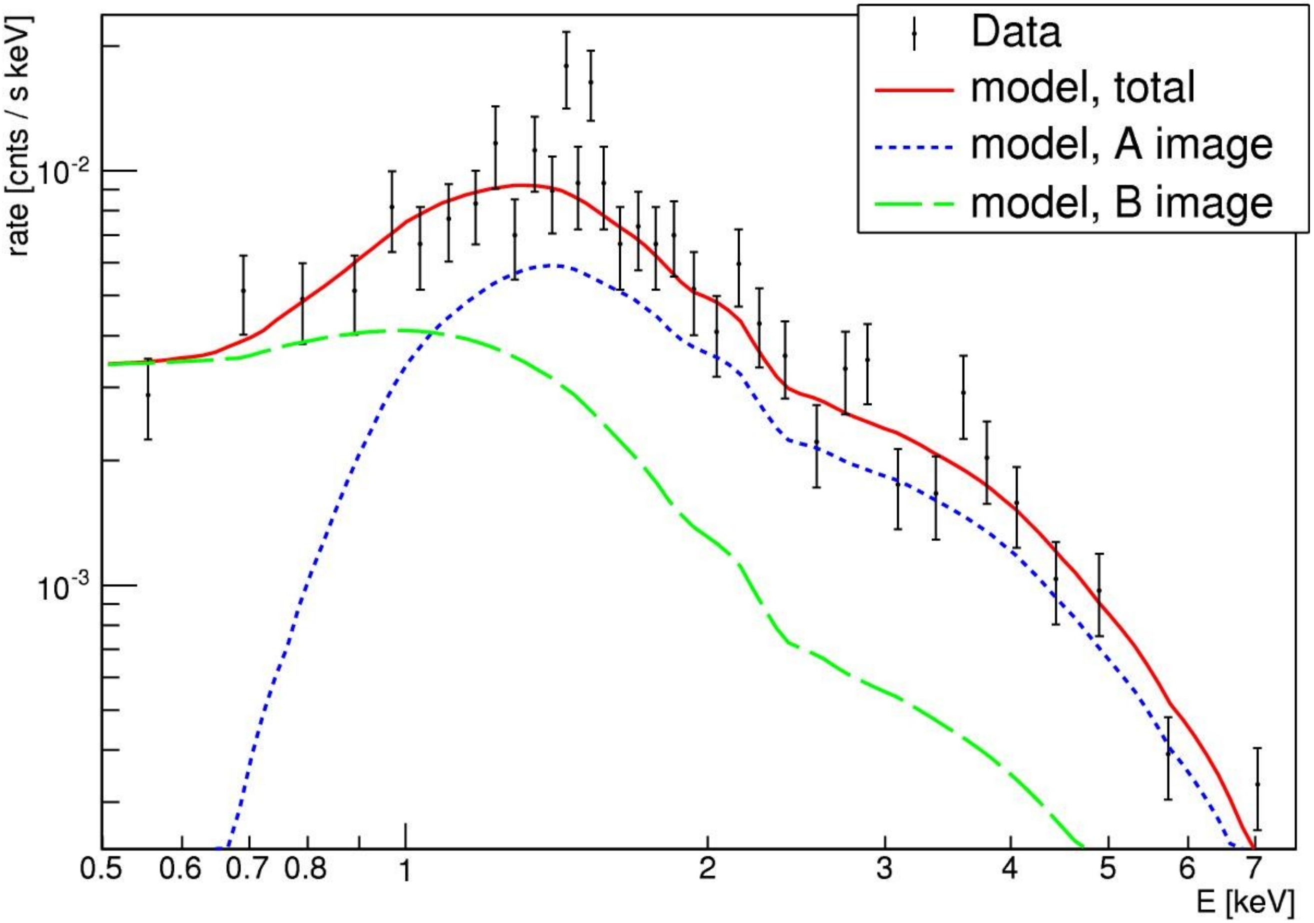

SED obtained during all the observations. Observed emission sum of the two images of the source. X-ray spectrum modeled as sum of two power-law components with magnifications fixed to 2.7 and 0.7 (and with the assumption that absorption affect only the leading image).

Spectral Results - *Swift*

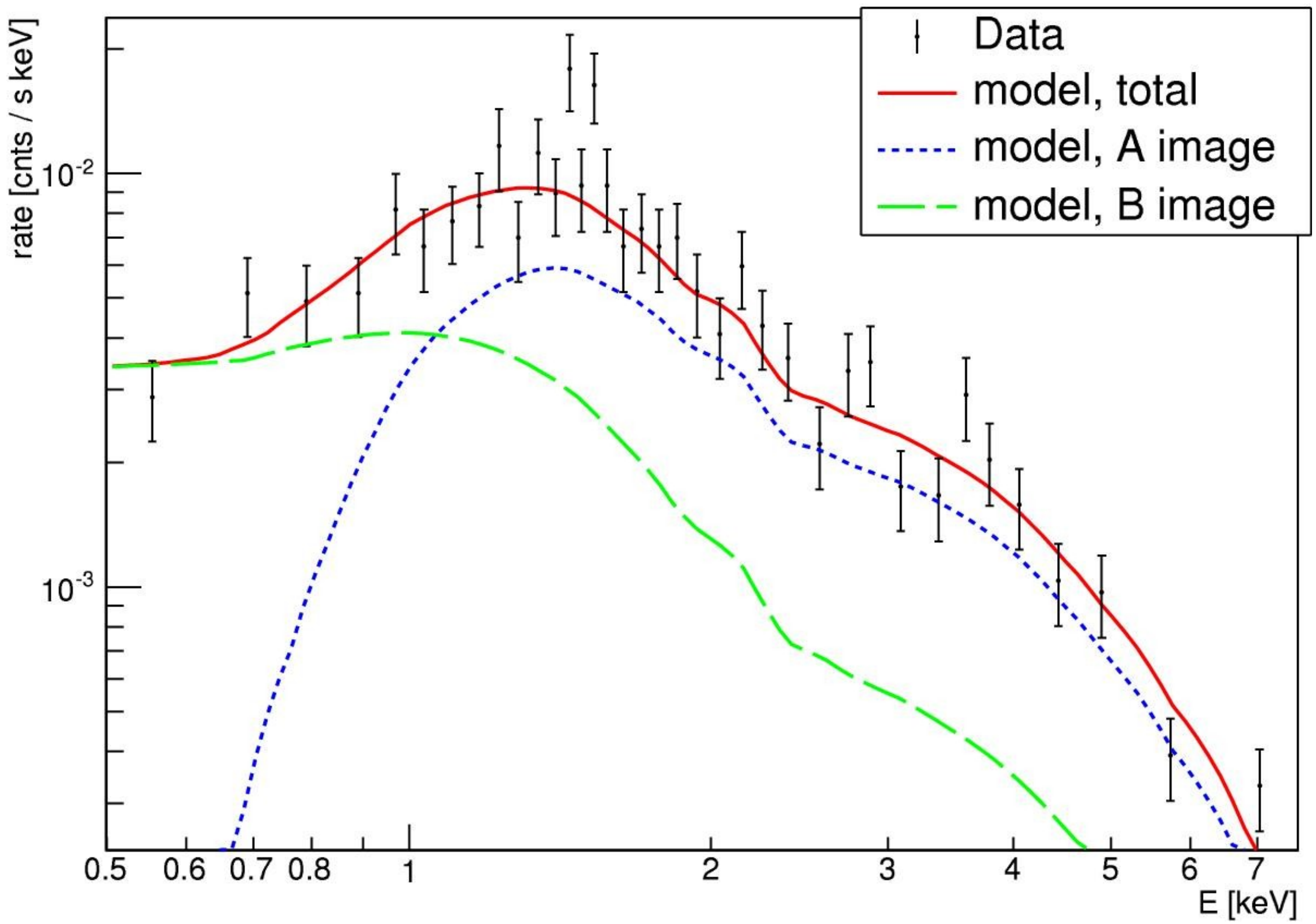

$$\frac{dN}{dE} = f_0 \times \left(\frac{E}{1keV}\right)^{-\gamma} [cm^{-2}s^{-1}keV^{-1}]$$

$$f_0 = (2.69 \pm 0.29) \times 10^{-4} cm^{-2}s^{-1}keV^{-1}$$
$$\gamma = 1.90 \pm 0.08$$

Broadband emission

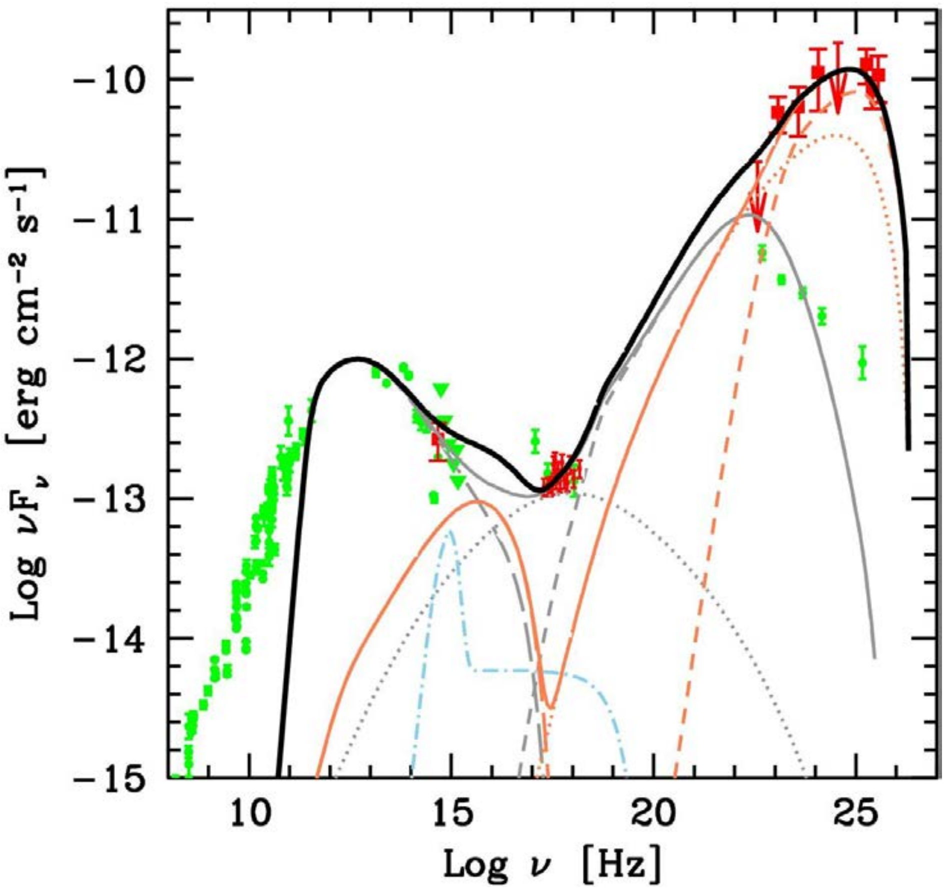

- Modelling dependent on the different magnification factor at different energies
  - Optical: $\mu_T \sim \mu_{trail}$ (strong absorption)
  - Xray: $\mu_T \sim \mu_{trail} + \mu_{lead} \sim 3.4$ (low variability and no strong absorption)
  - VHE: $\mu_T \sim \mu_{trail}$ (strong variability and much harder GeV spectrum during MAGIC observation)
- Broadband SED demagnified according to the numbers derived above and corrected for the optical, X-ray and gamma-ray absorption.
- Green points: Historical data
- Red points: Data taken during the flaring event.
- SED dominated by the emission in the GeV - sub-TeV energies, with not a similar increase at lower energies (unusual).

Broadband emission

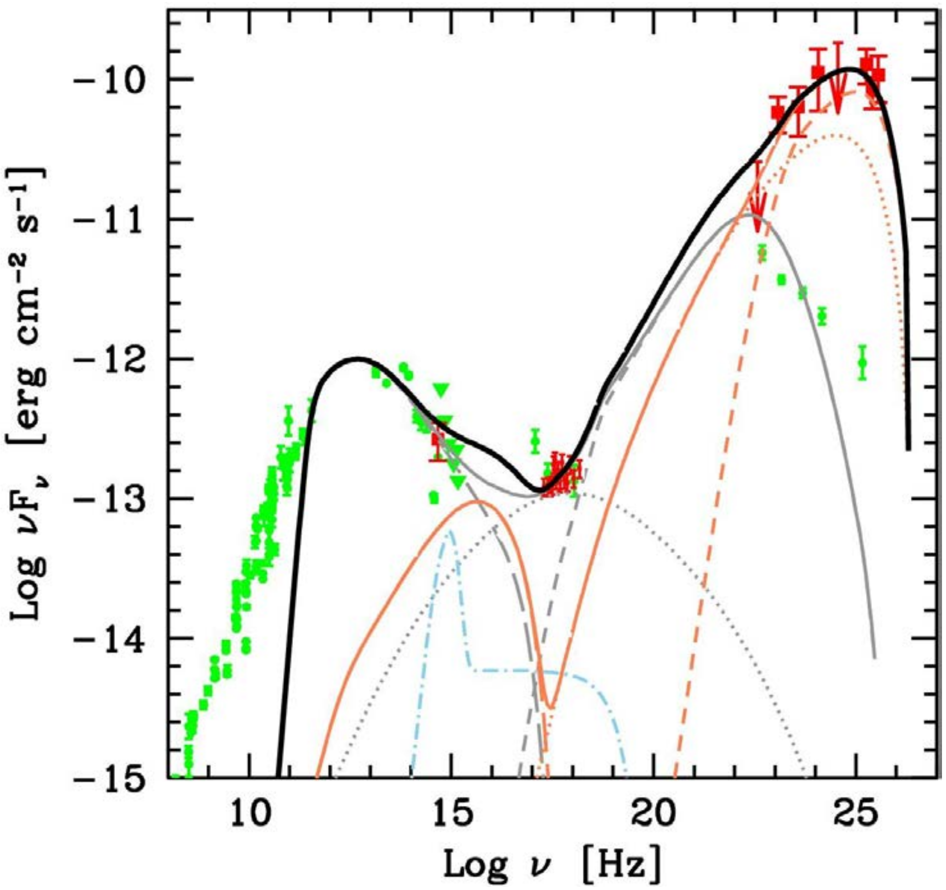

One zone leptonic models

- One zone scenario: e- emitting synchrotron radiation in the lower energy range and photons partly upscattered to VHE by inverse compton on the same e- (SSC).
- In order to obtain such a large separation between the two peaks the Doppler factors need to be high and the magnetic field very low. But with a large Doppler factor is unlikely that the radiation energy density in the jet frame could be dominated by synchrotron energy density.
- More plausilble that VHE component produced by the scattering of external photons (from BLR). Unfortunatly this scenario needed again a large Doppler factor.
- Due to the extremely large values of the Doppler factors, plus the lack of simultaneous optical and X-ray variability to the GeV and sub-TeV flare, strongly disfavor one-zone models.

Broadband emission

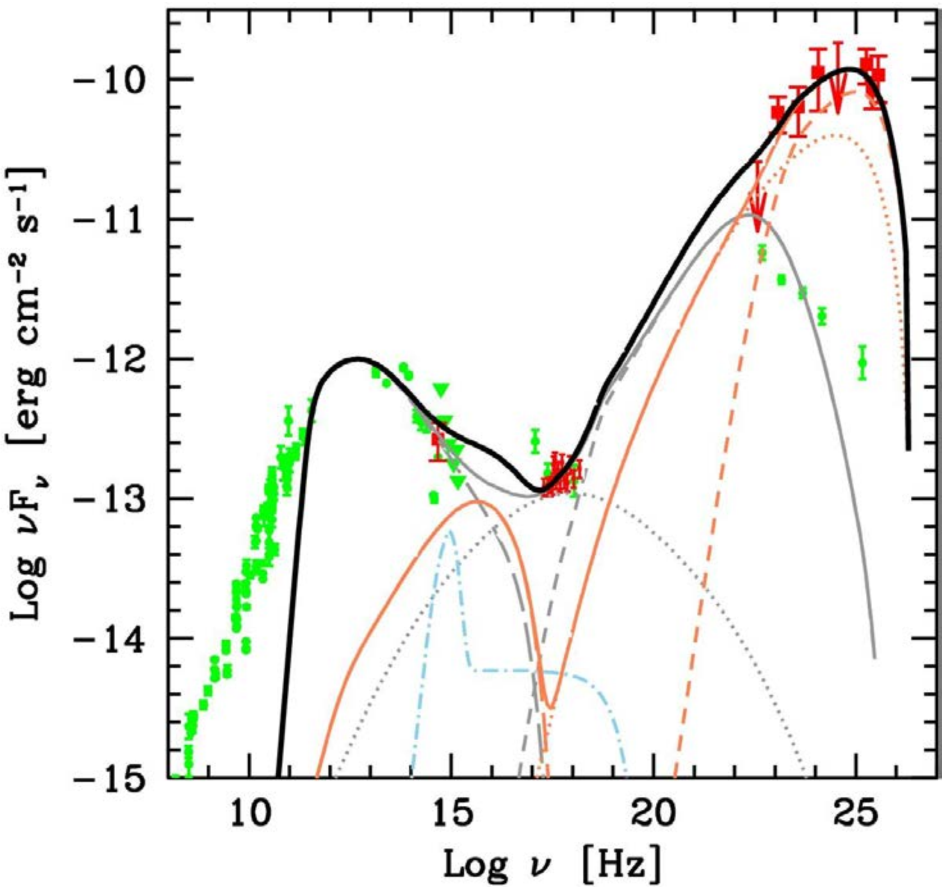

Two zone external Compton model

- Two different emissions regions moving with the same Doppler factor along the jet. Assumption: First emission region inside BLR, while the second one (producing VHE photons) outside BLR.
- Gamma-ray emission is the sum of SSC and EC components on the two different regions (but in farther region these processes are more efficient).
- $L_D = 6\times10^{44}$ erg s^{-1}, $R_{BLR} = 7.7\times10^{16}$ cm, $R_{torus} = 2\times10^{18}$ cm → 1 day variability time scale
- Low variability in Optical/X-ray points to a stability of the emission in the inner region.
- Again low magnetic field needed (in the outer region). Maybe some processes involving magnetic reconnection?

EBL constrains

$$\left(\frac{dN}{dE}\right)_{obs} = \left(\frac{dN}{dE}\right)_{int} \times exp(-\alpha \times \tau(E,z))$$

$$\left(\frac{dN}{dE}\right)_{int,PWL} = AE^{-\gamma}$$

$$\left(\frac{dN}{dE}\right)_{int,PWLcut} = AE^{-\gamma}exp(-E/E_{cut})$$

$$\left(\frac{dN}{dE}\right)_{int,LP} = AE^{-\gamma-b\log E}$$

$$\left(\frac{dN}{dE}\right)_{int,LPcut} = AE^{-\gamma-b\log E}exp(-E/E_{cut})$$

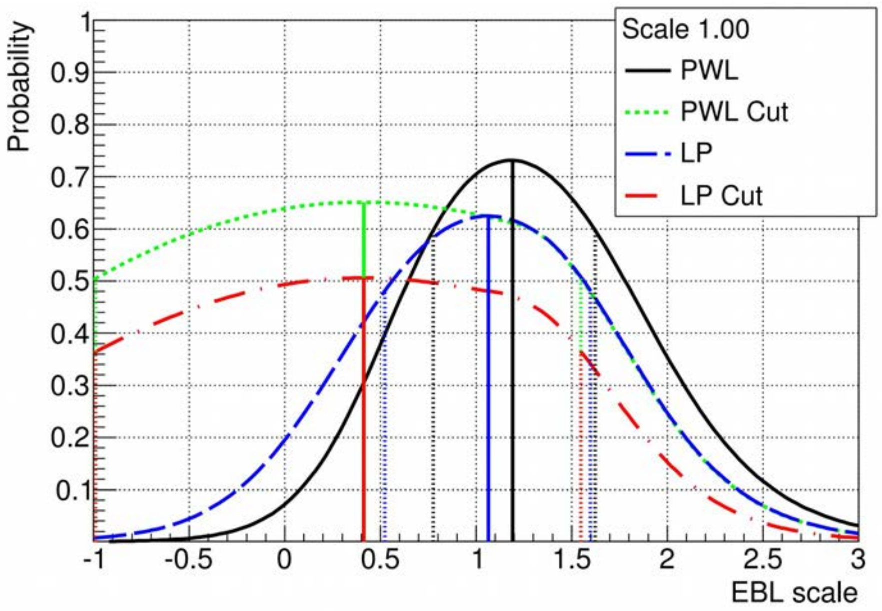

- Indipendent measurment of EBL absorption at z=0.944 with Fermi-LAT and MAGIC data.
- GeV and sub-TeV emission originates from same emission region.
- Joint spectral fit using a set of possible spectral shapes. Intrinsical shapes attenued by EBL according to optical depths by Domínguez et al. 2011 (plus an additional scaling parameter α of the optical depth).
- Highest fit probability obtained with simple PWL spectral model and an $\alpha=1.19\pm0.42_{stat}\pm0.25_{syst}$.
- Systematic effect due to the 15% uncertainty of the energy scale of MAGIC.
- Analysis repeated with other current EBL models (Franceschini et al. 2008, Finke et al. 2010, Gilmore et al. 2012, Inoue et al. 2013). The combined Fermi/MAGIC spectra is consistent with all five EBL models.

Conclusions

- MAGIC has detected VHE gamma-ray emission from QSO B0218+357 during the trailing component of a flare in July 2014.

- VHE emission lasted for two nights achieving the observed flux of about ~30% of Crab Nebula at 100 GeV. Intrinsic spectral index (using EBL model from Domínguez et al. 2011) found to be 2.35+-0.75$_{stat}$+-0.20$_{syst}$.

- VHE flare was not accompained by a simultaneous flux increase in the optical or X-ray energy range.

- Combined Fermi-LAT and MAGIC energy spectrum is consistent with current EBL models (but with not very strong constrains)

- Broadband emission modeled in the framework of a two-zone external Compton model. Quasi-stable optical and X-ray emission originate mostly in the inner zone. Enhanced gamma-ray emission produced outside the BLR.

THANKS FOR YOUR ATTENTION!!!